p90 ribosomal S6 kinase 2 exerts a tonic brake on G protein-coupled receptor signaling

Douglas J. Sheffler*, Wesley K. Kroeze*, Bonnie G. Garcia†, Ariel Y. Deutch†, Sandra J. Hufeisen*, Patrick Leahy‡§, Jens C. Brüning¶, and Bryan L. Roth*‡‖**††

Departments of *Biochemistry, ‖Neurosciences, and **Psychiatry, and ‡Comprehensive Cancer Center, Case Western Reserve University School of Medicine, Cleveland, OH 44106; †Departments of Psychiatry and Pharmacology, Vanderbilt University Medical Center, Nashville, TN 37212; §University Hospitals of Cleveland, Cleveland, OH 44106; and ¶Institute for Genetics and Center for Molecular Medicine, University of Cologne, Zülpicher Strasse 47, D-50674 Cologne, Germany

Communicated by Erminio Costa, University of Illinois, Chicago, IL, January 23, 2006 (received for review November 1, 2005)

G protein-coupled receptors (GPCRs) are essential for normal central CNS function and represent the proximal site(s) of action for most neurotransmitters and many therapeutic drugs, including typical and atypical antipsychotic drugs. Similarly, protein kinases mediate many of the downstream actions for both ionotropic and metabotropic receptors. We report here that genetic deletion of p90 ribosomal S6 kinase 2 (RSK2) potentiates GPCR signaling. Initial studies of 5-hydroxytryptamine (5-HT)$_{2A}$ receptor signaling in fibroblasts obtained from RSK2 wild-type (+/+) and knockout (−/−) mice showed that 5-HT$_{2A}$ receptor-mediated phosphoinositide hydrolysis and both basal and 5-HT-stimulated extracellular signal-regulated kinase 1/2 phosphorylation are augmented in RSK2 knockout fibroblasts. Endogenous signaling by other GPCRs, including P2Y-purinergic, PAR-1-thrombinergic, β1-adrenergic, and bradykinin-B receptors, was also potentiated in RSK2-deficient fibroblasts. Importantly, reintroduction of RSK2 into RSK2−/− fibroblasts normalized signaling, thus demonstrating that RSK2 apparently modulates GPCR signaling by exerting a "tonic brake" on GPCR signal transduction. Our results imply the existence of a novel pathway regulating GPCR signaling, modulated by downstream members of the extracellular signal-related kinase/mitogen-activated protein kinase cascade. The loss of RSK2 activity in humans leads to Coffin–Lowry syndrome, which is manifested by mental retardation, growth deficits, skeletal deformations, and psychosis. Because RSK2-inactivating mutations in humans lead to Coffin–Lowry syndrome, our results imply that alterations in GPCR signaling may account for some of its clinical manifestations.

serotonin | signal transduction

G protein-coupled receptors (GPCRs) represent proximal molecular targets for most neurotransmitters, many psychiatric medications, and some drugs of abuse (1). Thus, for instance, antipsychotic and antidepressant medications interact with literally dozens of GPCRs (2). Drugs of abuse tend to have a more restricted pattern of interaction, with morphine being selective for μ-opioid receptors, and salvinorin A being selective for κ-opioid sites (3). GPCRs can also function as coreceptors for viruses; thus, the 5-hydroxytryptamine (5-HT)$_{2A}$ serotonin receptor acts as a coreceptor for the JC virus, the agent responsible for progressive multifocal leukoencepalpathy (4). Agonist-induced activation of GPCRs frequently leads to a complex cascade of intracellular signaling involving arrestins and members of the mitogen-activated protein kinase (MAPK) cascade (5).

The p90 ribosomal S6 kinases (RSK)1–4 are downstream members of the extracellular signal-regulated kinase (ERK)/MAPK cascade, which contain two separate kinase domains connected by a linker domain (Fig. 1*B*) (6). Multiple phosphorylation events by upstream protein kinases are necessary for the complete activation of the N-terminal kinase (NTK) domain of RSKs (Fig. 1*B*). The NTK of RSK2 phosphorylates a broad range of substrates, including cAMP response element-binding protein, c-Fos, IκB/NF-κB, glycogen synthase kinase-3, and many others (7). Because RSK2 has a broad range of substrates and actions, it is likely to participate in many other cellular processes. Intriguingly, RSK2 has also been found in association with NMDA and α-amino-3-hydroxy-5-methyl-4-isoxazolepropionic acid (AMPA) receptors (8, 9), which also interact with postsynaptic density protein 95 (10) and have been implicated in the etiology of psychotic disorders (11). Recently, RSK2 has also been demonstrated to regulate excitatory synaptic transmission via AMPA receptors (9).

Coffin–Lowry syndrome (CLS) is an X-linked mental retardation syndrome resulting from null mutations of RSK2 (12). CLS is characterized by severe mental retardation, craniofacial and skeletal deformities, growth retardation, movement and cardiovascular disorders, and a schizophrenia-like psychosis in heterozygotic females (6). RSK2 knockout mice show diminished memory, coordination deficits, and growth retardation (13), providing a model for the study of CLS. In addition, RSK2 knockout mice demonstrate alterations in insulin- and exercise-stimulated ERK/MAPK signal transduction (13) and in transcription factor phosphorylation (14). Because the transcription factor cAMP response-element-binding protein (CREB) is implicated in learning and memory (15), changes in the CREB pathway associated with RSK2 deficiency may lead, in part, to the symptoms of CLS.

We report here that RSK2 also has a regulatory function on GPCR signaling exerting a "tonic brake" on second-messenger production for a number of GPCRs. These results imply the existence of a previously uncharacterized pathway regulating GPCR signaling, modulated by downstream members of the ERK/MAPK cascade.

Results

Identification of RSK2 as a 5-HT$_{2A}$ Receptor-Interacting Protein. As part of a larger effort to identify novel GPCR regulators, we performed a yeast two-hybrid screen of a human brain cDNA library (see *Supporting Text*, which is published as supporting information on the PNAS web site) using the third intracellular loop (i3) of the 5-HT$_{2A}$ receptor as bait. A large number of putative 5-HT$_{2A}$ receptor-interacting proteins were identified (see Table 2, which is published as supporting information on the PNAS web site, for details) and one clone, 33.5, which encoded a portion of the C-terminal kinase domain of RSK2, was selected for further study (Fig. 1 *A* and *B*; Table 2).

The site of interaction between RSK2 and the 5-HT$_{2A}$ receptor i3 loop bait was identified by making serial deletions of the i3 loop and monitoring the interaction with the RSK2 target by two-hybrid

NEUROSCIENCE

Conflict of interest statement: No conflicts declared.

Abbreviations: GPCR, G protein-coupled receptor; MAPK, mitogen-activated protein kinase; RSK, p90 ribosomal S6 kinase; ERK, extracellular signal-regulated kinase; 5-HT, 5-hydroxytryptamine; HEK, human embryonic kidney; FLAG-5-HT$_{2A}$, human FLAG-tagged 5-HT$_{2A}$ receptor; PI, phosphoinositide; i3, third intracellular loop; CLS, Coffin–Lowry syndrome.

††To whom correspondence should be addressed. E-mail: bryan.roth@case.edu.

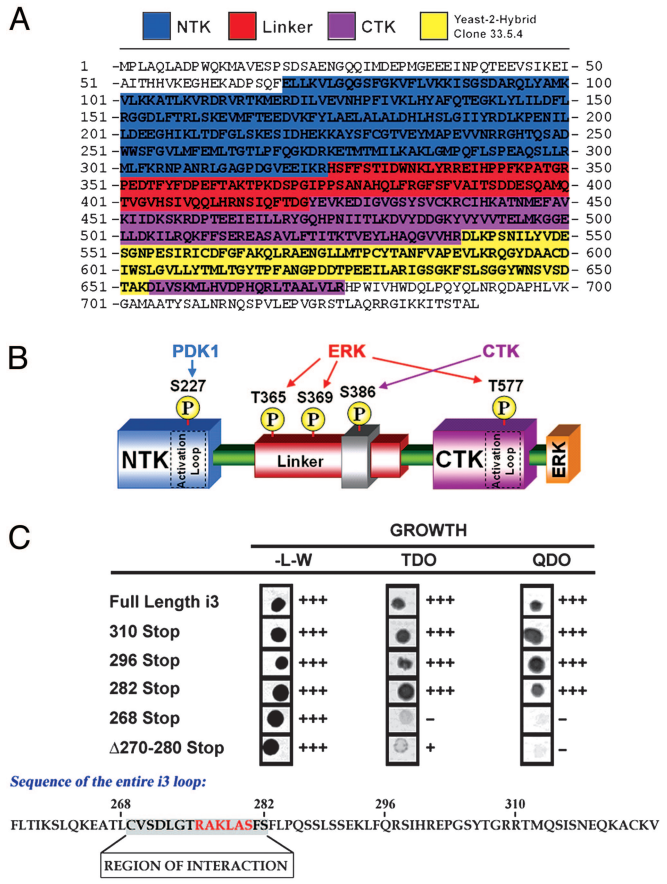

Fig. 1. RSK2 interacts with 5-HT_{2A} receptors. (*A*) Protein sequence of mouse RSK2 (GenBank accession no. NP_683747), with the N-terminal kinase (NTK) domain of RSK2 (blue), the linker domain (red), the C-terminal kinase (CTK) domain (purple), and the i3 loop-binding region identified in the yeast two-hybrid screen (yellow). (*B*) Domain structure of RSK2, residues phosphorylated in RSK2 activation, and kinases known to phosphorylate those residues. (*C*) Growth of yeast strain PJ69–2A cotransformed with truncation mutants of the i3 bait and the RSK2 target on quadruple or triple dropout media (see *Supporting Text* for details).

analysis (see *Supporting Text*). Fig. 1*C* shows that growth of yeast on triple dropout (TDO) and quadruple dropout (QDO) media was lost when the i3 loop was truncated to amino acid 268, but that growth still occurred with the amino acid 282 truncation. This was not a "length effect" of the truncation of the i3 loop, because the yeast also failed to grow on TDO and QDO when transformed with the full i3 loop containing a deletion of amino acids 270–280 and the RSK2 target. These findings identified RSK2's site of interaction with the 5-HT_{2A} receptor i3 loop to residues 270–280 of the 5-HT_{2A} receptor, a region that includes a putative RSK2 consensus phosphorylation site (amino acids 275–280; Fig. 1*C*).

Coimmunoprecipitation studies verified the 5-HT_{2A} receptor–RSK2 interaction *in vitro* and *in vivo*. For *in vitro* studies, human embryonic kidney (HEK)-293 cells were transiently transfected with human FLAG-tagged 5-HT_{2A} receptors (FLAG-5-HT_{2A}) and RSK2 (Fig. 2*A*). As shown in Fig. 2*A*, RSK2 was coimmunoprecipitated with FLAG-5-HT_{2A} receptors (Fig. 2*A*, lanes 3 and 4), indicating that 5-HT_{2A} receptors and RSK2 associate *in vitro*. The association of FLAG-5-HT_{2A} and RSK2 was unaltered by agonist exposure (Fig. 2*A*, compare lanes 3 and 4), indicating that 5-HT_{2A} receptors and RSK2 associate in an agonist-independent manner in HEK-293 cells. Coimmunoprecipitation studies were also done in two different cellular milieus where 5-HT_{2A} receptors and RSK2 are constitutively expressed (C6-glioma cells and rat brain synaptic membranes), to determine whether RSK2 and the 5-HT_{2A} receptor associate *in vivo*. To verify the specificity of the interaction, immunoprecipitations were performed by using protein-A/G agarose beads in the absence (−) or presence (+) of a monoclonal anti-RSK2 antibody. Fig. 2*B*, first image, shows that 5-HT_{2A}-like immunoreactivity was present in C6-glioma cell immunoprecipitates only when the RSK2 antibody was used (compare lanes 1 and 2). Fig. 2*B*, third image, shows the immunoprecipitation of RSK2 in the presence of the monoclonal RSK2 antibody but not with protein A/G beads alone, confirming the specificity of the immunoprecipitation. Fig. 2*B*, second and fourth images, shows that equivalent levels of 5-HT_{2A}-like immunoreactivity and RSK2 were present in the lysates from which the immunoprecipitations were performed. These data indicate that RSK2 and 5-HT_{2A} receptors endogenously associate in C6-glioma cells. Similar results were obtained by using rat brain synaptic membranes (Fig. 2*C*).

We also examined the distribution of RSK2 in rat brain in two regions rich in 5-HT_{2A} receptors: the prefrontal cortex and the globus pallidus. Fig. 2 *D–F* show that 5-HT_{2A} receptors and RSK2 were colocalized in the globus pallidus. Fig. 2 *G–I* show that 5-HT_{2A} receptors and RSK2 were also colocalized in layer V pyramidal neurons in the prefrontal cortex. Fig. 2 *J–L* show higher magnifications of layer V pyramidal neurons in the prefrontal cortex and indicate an overlapping and punctate distribution of 5-HT_{2A} receptors and RSK2. Together, these data show that 5-HT_{2A} receptors and RSK2 have overlapping cellular and subcellular distributions in rat brain.

RSK2 Modulates GPCR Signaling. To determine the functional significance of this interaction, we obtained fibroblasts from RSK2+/+ and RSK2−/− mice (14). We performed microarray studies to identify endogenously expressed GPCRs in these cell lines (Table 3, which is published as supporting information on the PNAS web site) and assessed signaling at a subset of the identified receptors. As shown in Fig. 3 *A–C* and Fig. 5, which is published as supporting information on the PNAS web site, deletion of RSK2 augments agonist-stimulated intracellular Ca^{2+} release for 5-HT_{2A}-serotonergic, P2Y-purinergic, and PAR1-thrombinergic receptors and also potentiated agonist-stimulated β1-adrenergic receptor cAMP accumulation.

We next examined 5-HT_{2A} receptor signaling in both cell lines in greater detail. In both RSK2−/− and RSK2+/+ fibroblasts, 5-HT induced an increase in phosphoinositide (PI) accumulation that was abolished by the selective 5-HT_{2A} antagonist (2,3-dimethoxyphenyl)-[1-[2-fluorophenyllethyl]-4-piperidyl]methanol (MDL100,907) (Fig. 3*D*), indicating that RSK2−/− and RSK2+/+ fibroblasts express functional 5-HT_{2A} receptors. Quantitative RT-PCR studies (see *Supporting Text* for details) disclosed that both cell lines expressed equivalent amounts of 5-HT_{2A} mRNA (Fig. 3*E*). We also found that 5-HT_{2A}-mediated PI hydrolysis was augmented in the RSK2−/− fibroblasts (Fig. 3*D*). To determine whether this was due to an enhanced surface expression of 5-HT_{2A} receptors, we prepared stable lines expressing FLAG-5-HT_{2A} and performed surface biotinylation studies. We found that stable lines of RSK2−/− and RSK2+/+ fibroblasts overexpressing FLAG-5-HT_{2A} receptors displayed enhanced 5-HT_{2A}-mediated maximal PI accumulation (Fig. 3*F*), but no difference in the cell surface expression of FLAG-5-HT_{2A} receptors (as determined by cell surface biotinylation) was measured (Fig. 3*G*). These data indicate that the alterations in signaling are not due to differences in 5-HT_{2A} receptor expression.

Microarray studies were used to determine whether the changes in GPCR signaling might be due to altered expression of genes involved in second-messenger production. Similar numbers of genes were expressed ["present" calls by the Affymetrix software (see *Dataset1*, which is published as supporting information on the PNAS web site); see *Supporting Text* for details] in the RSK2+/+ and RSK2−/− fibroblasts, and roughly equivalent numbers of

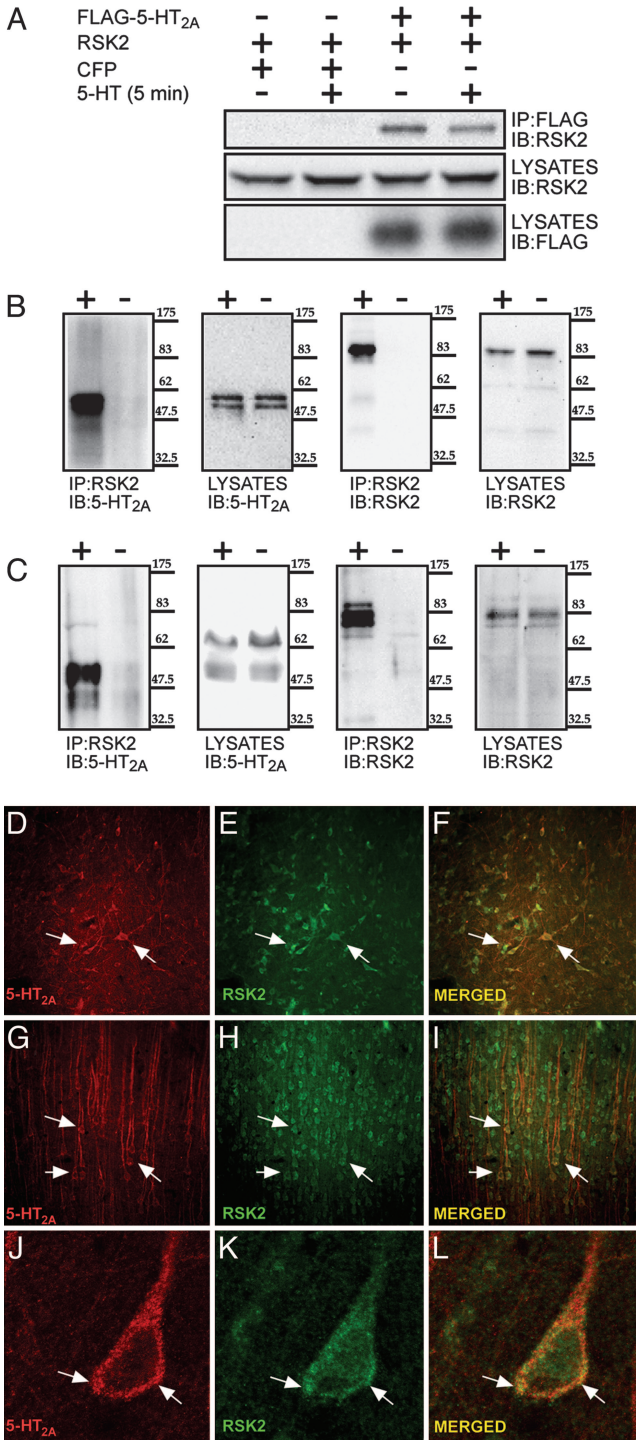

Fig. 2. RSK2 interacts with 5-HT_{2A} receptors *in vitro* and *in vivo*. (*A*) Coimmunoprecipitation of RSK2 with FLAG-5-HT_{2A} receptors in transfected HEK-293 cells. HEK-293 cells were transiently cotransfected with either RSK2 and cyan fluorescent protein (CFP) (negative control) (lanes 1 and 2) or FLAG-5-HT_{2A} and RSK2 (lanes 3 and 4). Protein lysates were prepared, and equivalent amounts of protein were loaded for all sets. Lanes 1 and 3 were treated with vehicle, and lanes 2 and 4 were treated with 10 μM 5-HT for 5 min. FLAG-tagged human 5-HT_{2A} receptors were immunoprecipitated (IP) by a monoclonal FLAG antibody conjugated to Sepharose beads. (*B*) Coimmunoprecipitation of native 5-HT_{2A} receptors with RSK2 in C6-glioma cells. (*C*) Coimmunoprecipitation of native 5-HT_{2A} receptors with RSK2 from rat brain synaptic membrane preparations. For experiments in native cell lines, cell lysates were prepared from either C6-glioma cells (*B*) or rat brain synaptic membranes (*C*), and equivalent amounts of protein were loaded for all sets. In both *B* and *C*, the first image shows that native 5-HT_{2A} receptors are immunoprecipitated by monoclonal RSK2 antibody (lane 1 [+]) by using protein A/G beads but not protein A/G beads alone (lane 2 [−]). The second image shows native 5-HT_{2A} receptors present in the lysates (lanes 1 and 2). The third image shows robust RSK2 detection in the immunoprecipitate in the presence of RSK2 antibody (lane 1 [+]) but not with protein A/G beads alone (lane 2 [−]). The fourth image shows RSK2 in the lysates (lanes 1 and 2). Shown are representative immunoblots (IB) from a single experiment since replicated three times with similar results. (*D–L*) Rat brain sections were prepared and stained as described in *Materials and Methods*, followed by dual-label immunofluorescent confocal microscopy. Representative images from one of three independent experiments are shown. (*D–F*) Globus pallidus. (*G–I*) Layer V prefrontal cortex. (*J–L*) Higher-power layer V prefrontal cortex. Native rat 5-HT_{2A} receptors are shown in the red channel (*D*, *G*, and *J*), and native rat RSK2 is shown in the green channel (*E*, *H*, and *K*). The merged images are in *F*, *I*, and *L*.

genes were "increased" and "decreased" when RSK2−/− and RSK2+/+ fibroblasts were compared (data not shown). Additionally, 97% of the expressed genes showed <2-fold changes between RSK2+/+ and RSK2−/− lines. Taken together, we interpret these findings to indicate that no global change in gene expression occurs in the absence of RSK2 (see *Supporting Text* and Fig. 6, which is published as supporting information on the PNAS web site). However, there were selected alterations in gene expression of pathways in which RSK2 has been well characterized to play a role, such as cell cycle progression (see Fig. 7, which is published as supporting information on the PNAS web site, and *Supporting Text* for full details). Importantly, however, no changes in gene expression were seen for members of GPCR signal transduction cascades (Fig. 8, which is published as supporting information on the PNAS web site) that would account for the augmented signaling phenotype. These data indicate that the augmented signaling in RSK2−/− fibroblasts was not due to alterations in the expression of genes that regulate GPCR second-messenger production.

We next examined in greater detail the augmented signaling caused by RSK2 knockout and found an effect on maximal second-messenger production but no change in agonist potency for any of the receptors examined (Fig. 4 and Table 1). To verify that the signaling differences between RSK2+/+ and RSK2−/− fibroblasts were due to the absence of RSK2 in the knockout cells and to mouse strain background differences or phenotypic drift, several monoclonal lines were prepared in which RSK2 was stably reintroduced into the RSK2−/− fibroblast background. Fig. 4*A* shows the expression of RSK2 in the RSK2−/− and RSK2+/+ fibroblasts and in the RSK2−/− RSK2-transfected stable line. Reintroduction of RSK2 into the RSK2−/− background reversed the PI hydrolysis phenotype for 5-HT_{2A}-serotonergic, PAR-1-thrombinergic, bradykinin-B, and P2Y-purinergic receptor-mediated signaling (Fig. 4 *B–E*). Thus, reintroduction of RSK2 into RSK2−/− fibroblasts normalizes signaling.

To determine whether the augmentation of 5-HT_{2A} receptor-mediated PI hydrolysis in the absence of RSK2 was due to differences in receptor phosphorylation, [^{32}P]orthophosphate metabolic labeling studies were performed (see *Supporting Text* for details). Fig. 4*F* shows a representative immunoblot and autoradiogram of cells metabolically labeled with [^{32}P]orthophosphate, followed by immunoprecipitation of FLAG-5-HT_{2A} receptors. As reported (16), 5-HT_{2A} receptors were not detectably phosphorylated. These data imply that differences in 5-HT_{2A} receptor signaling in RSK2−/− and RSK2+/+ fibroblasts may not be due to differences in phosphorylation of 5-HT_{2A} receptors, although further studies will be needed to definitively address this possibility.

RSK2 Modulates ERK1/2 Phosphorylation. Finally, we examined 5-HT_{2A} receptor-stimulated ERK1/2 phosphorylation in response to 5-HT. We found that both basal (0-min) and 5-HT stimulated (5-, 10-, 15-, and 30-min) ERK1/2 phosphorylation was increased in RSK2−/− compared with RSK+/+ fibroblasts (Fig. 9 *A* and *B*,

NEUROSCIENCE

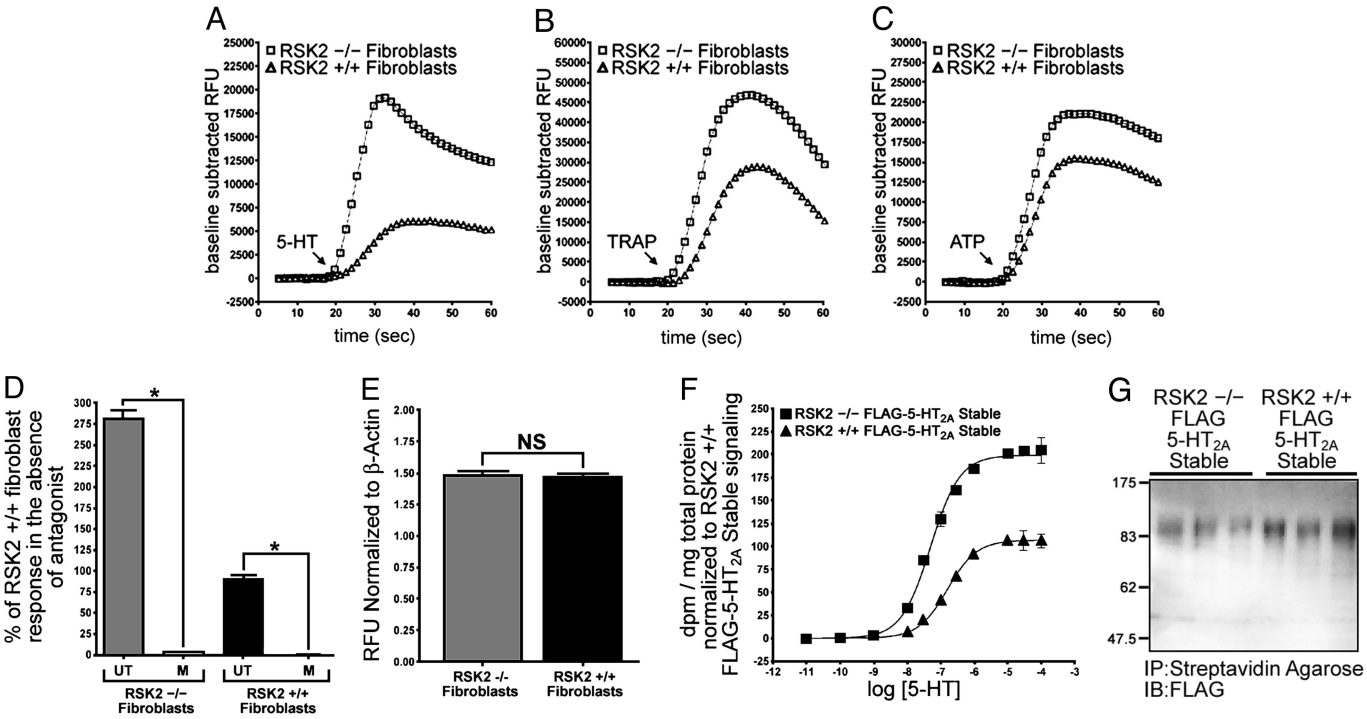

Fig. 3. RSK2 knockout augments the signaling of 5-HT_{2A}-serotonergic, PAR-1-thrombinergic, and P2Y-purinergic receptors. (*A–C*) For these studies, RSK2+/+ and RSK2−/− fibroblasts were plated onto 96-well plates. Cells were serum-starved, treated with agonist at the 20-sec time point, and calcium mobilization was measured as described in *Supporting Text*. (*A*) Representative tracing of the changes in fluorescence of RSK2−/− and RSK2+/+ fibroblasts upon addition of 1 nM 5-HT. (*B*) Representative tracing of the changes in fluorescence of RSK2−/− and RSK2+/+ fibroblasts upon addition of 1 μM thrombin receptor-activating peptide. (*C*) Representative tracing of the changes in fluorescence of RSK2−/− and RSK2+/+ fibroblasts upon addition of 10 μM ATP. (*D*) RSK2+/+ and −/− fibroblasts were plated and treated as described in *Materials and Methods*, and maximal PI hydrolysis was measured in the presence (M) and absence (UT) of 100 nM MDL100,907. (*E*) Quantitative RT-PCR for the 5-HT_{2A} receptor normalized to β-actin levels, indicating that both the RSK2+/+ and RSK2−/− fibroblasts express similar levels of 5-HT_{2A} mRNA. (*F*) RSK2+/+ FLAG-5-HT_{2A} stable line and RSK2−/− FLAG-5-HT_{2A} stable line fibroblasts were plated onto 24-well plates. PI accumulation upon agonist exposure was measured as outlined in *Materials and Methods*. (*G*) A representative immunoblot (IB) of cell surface FLAG-5-HT_{2A} receptors in the RSK2+/+ FLAG-5-HT_{2A} stable line and in the RSK2−/− FLAG-5-HT_{2A} stable line as determined by cell surface biotinylation as outlined in *Materials and Methods*. IP, immunoprecipitation.

which is published as supporting information on the PNAS web site). Significantly, the elevated basal levels of ERK1/2 phosphorylation were attenuated by treatment with 100 nM MDL100,907 (Fig. 9*A*, compare lanes M and 0; Fig. 9*C*), a highly selective 5-HT_{2A} antagonist (17). These results imply that the increase in basal phosphorylation seen in RSK2−/− fibroblasts is due, at least in part, to augmented constitutive 5-HT_{2A} receptor activity.

Discussion

In this paper, we show that RSK2 exerts a tonic brake on GPCR signaling. We also show that RSK2 can directly interact with at least one GPCR (the 5-HT_{2A} serotonin receptor), and that this association has two significant cellular consequences on GPCR signaling. The absence of RSK2 results first in an increase in agonist efficacy as measured through PI hydrolysis, without a change in agonist potency and second, in an increase in both basal and stimulated ERK phosphorylation. Intriguingly, this increase in basal ERK phosphorylation is attenuated by treatment with MDL100,907, a selective 5-HT_{2A} antagonist. Additionally, reintroduction of RSK2 into RSK2 knockout fibroblasts normalizes 5-HT_{2A} serotonin, PAR-1 thrombin, P2Y-purinergic, and bradykinin-B receptor-mediated signaling. Together, these findings describe a previously undescribed mode of GPCR regulation.

We have previously shown an interaction of 5-HT_{2A} receptors with postsynaptic density protein 95 (PSD-95), a PSD-95/discs large/ZO-1 (PDZ) domain-containing scaffolding protein that interacts with the extreme C-terminal tail of the 5-HT_{2A} receptor via a canonical type 1 PDZ ligand (18). In addition, a number of other GPCRs have previously been shown to interact with PDZ domain-containing scaffolding proteins (see ref. 19 for review).

Table 1. RSK2 knockout augments GPCR signaling

	Agonist potency, EC_{50} (pEC_{50} ± SEM)			Relative agonist efficacy, E_{max} ± SEM		
	RSK2−/− fibroblast	RSK2+/+ fibroblast	RSK2−/− RSK2 stable	RSK2−/− fibroblast	RSK2+/+ fibroblast	RSK2−/− RSK2 stable
5-HT_{2A}	678 nM (6.17 ± 0.16)	668 nM (6.18 ± 0.06)	568 nM (6.25 ± 0.17)	2.72 ± 0.19*	0.99 ± 0.03	1.53 ± 0.11*
PAR-1	8.6 μM (5.07 ± 0.10)	16.9 μM (4.78 ± 0.09)	6.3 μM (5.21 ± 0.06)	11.77 ± 0.70*	1.16 ± 0.08	8.37 ± 0.24*
P2Y	8.6 μM (5.06 ± 0.24)	6.0 μM (5.22 ± 0.09)	6.2 μM (5.21 ± 0.22)	3.22 ± 0.34*	0.98 ± 0.04	1.83 ± 0.16*
Bradykinin-B	0.19 nM (9.72 ± 0.40)	1.31 nM (8.88 ± 0.11)	0.26 nM (9.59 ± 0.27)	3.83 ± 0.40*	0.91 ± 0.11	1.06 ± 0.11

Agonist potencies (EC_{50}) and efficacies (E_{max}) were determined for agonist-mediated activation of PI hydrolysis, as described in *Materials and Methods*. pEC_{50} values are represented as −log of EC_{50} as molar concentrations. The results represent the average of four independent experiments.
*Statistically different from RSK2+/+ fibroblasts, $P < 0.05$.

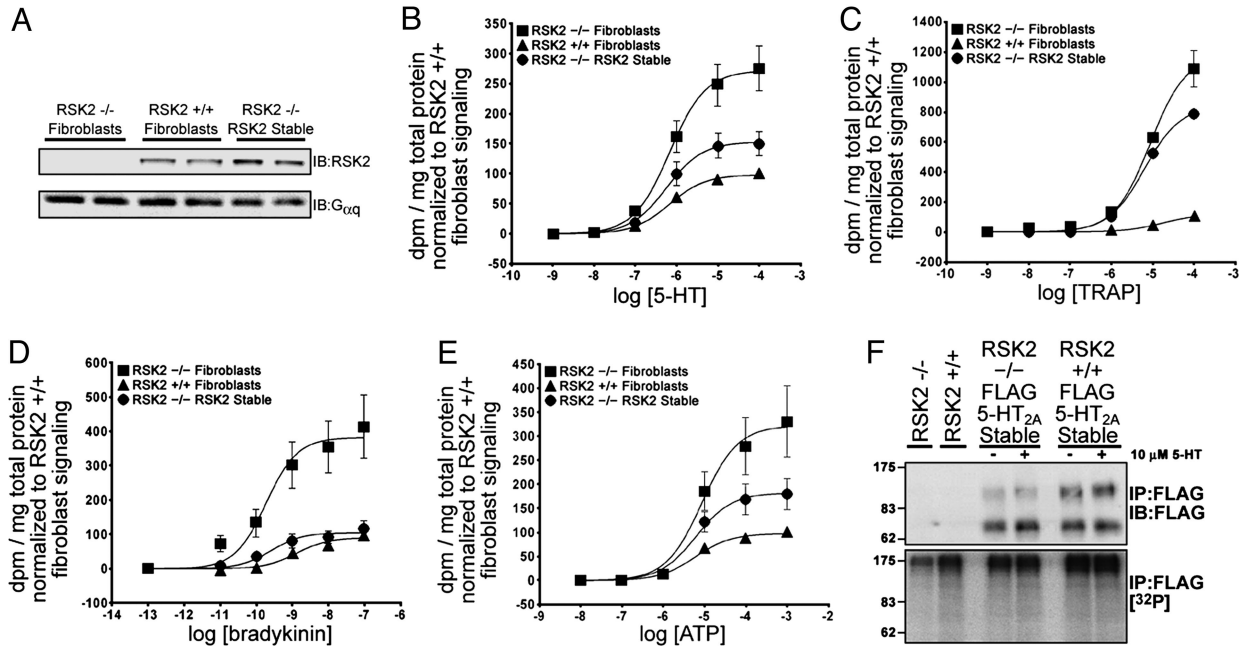

Fig. 4. RSK2 exerts a tonic brake on GPCR signaling. (*A*) The expression of RSK2 in the RSK2−/− fibroblasts, in the RSK2+/+ fibroblasts, and in the RSK2−/− RSK2-transfected stable line. (*B*) PI hydrolysis responses to various concentrations of 5-HT in RSK2−/− and RSK2+/+ fibroblasts and in RSK2−/− fibroblasts stably transfected with wild-type RSK2. (*C*) PI hydrolysis responses to various concentrations of TRAP in RSK2−/− and RSK2+/+ fibroblasts and in RSK2−/− fibroblasts stably transfected with wild-type RSK2. (*D*) PI hydrolysis responses to various concentrations of bradykinin in RSK2−/− and RSK2+/+ fibroblasts and in RSK2−/− fibroblasts stably transfected with wild-type RSK2. (*E*) PI hydrolysis responses to various concentrations of ATP in RSK2−/− and RSK2+/+ fibroblasts and in RSK2−/− fibroblasts stably transfected with wild-type RSK2. PI hydrolysis data are normalized to dpm per mg of total protein with RSK2+/+ fibroblast maximal signaling adjusted to 100%. (*F Upper*) A representative immunoblot of immunoprecipitated FLAG-5-HT_{2A} receptors. (*F Lower*) A representative autoradiogram of cells metabolically labeled with [^{32}P]orthophosphate followed by FLAG immunoprecipitation (IP) of FLAG-5-HT_{2A} receptors. IB, immunoblot.

Interestingly, RSK2 has recently been demonstrated to contain C-terminal sequences that bind PDZ domains, and the interaction of RSK2 with PDZ domain-containing proteins has been demonstrated to be important for the role of RSK2 in synaptic function (9). The possibility that PDZ domain-containing proteins, GPCRs, and RSK2 form large synaptic signaling complexes is an intriguing possibility that warrants further study. To this end, we will attempt to identify other RSK2-interacting proteins in future studies.

Prior studies with RSK2 knockout mice revealed an increase in basal or insulin- and exercise-stimulated ERK1/2 phosphorylation (13). Dufresne *et al.* (13) hypothesized that the augmented basal ERK1/2 phosphorylation could be due to either diminished feedback inhibition of RSK2 on the ERK/MAPK cascade or altered expression of one of the ERK phosphatases. Our studies have demonstrated a similar finding, showing an apparent dissociation between agonist treatment and basal ERK1/2 phosphorylation and an increase in 5-HT-stimulated ERK1/2 phosphorylation in the absence of RSK2. However, we suggest that the increase in basal ERK1/2 phosphorylation in RSK2 knockout mice and cells might be due to the removal of a tonic brake on GPCR signaling. That pretreatment of RSK2−/− fibroblasts with the 5-HT_{2A} receptor-selective antagonist MDL100,907 lowered basal ERK1/2 phosphorylation to levels similar to those seen in the RSK2+/+ fibroblasts supports this notion. Additionally, microarray data indicate that global dysregulation of phosphatases or MAPK cascade members does not occur at the mRNA level (see Table 4 and Fig. 10, which are published as supporting information on the PNAS web site). These data argue that RSK2 may have a novel role in maintaining the appropriate level of basal ERK-MAP kinase cascade activity by suppressing basal and receptor-stimulated activity of 5-HT_{2A} receptors, and perhaps other GPCRs.

The kinases participating in the phosphorylation of 5-HT_{2A} receptors have proven elusive, despite the presence of >30 potential phosphorylation sites and the identification of serine and threonine residues involved in desensitization (16). To date, no agonist-directed phosphorylation of 5-HT_{2A} receptors has been reported, despite continued study (16). Indeed, the association of RSK2 with 5-HT_{2A} receptors appears to be agonist-independent, because agonist stimulation had no effect on the coimmunoprecipitation of RSK2 with 5-HT_{2A} receptors. It is therefore possible that RSK2 constitutively phosphorylates the 5-HT_{2A} receptor, a possibility we are currently investigating. Because 5-HT efficacy is increased in RSK2 knockout cells, it is also possible that constitutive phosphorylation of 5-HT_{2A} receptors in wild-type cells could interfere with G protein-coupling efficiency, leading to a "predesensitized" state of the receptor.

Individuals with CLS have an increased risk of cardiac abnormalities, including mitral, tricuspid, and aortic valve abnormalities, pulmonary and aortic root dilation, and cardiomyopathy, suggesting an indispensable role for RSK2 in cardiovascular function (20). PAR-1 thrombin receptors are highly expressed in the heart and have many cardiovascular functions (21). Additionally, the 5-HT_{2A} receptor is highly expressed in vascular smooth muscle, pulmonary artery, and cardiac tissues. Because RSK2 deletion augments 5-HT_{2A} and PAR-1 signaling, our findings imply that cardiovascular abnormalities in patients with CLS may be due to a hyperactivation of GPCR signaling.

In summary, RSK2 has emerged as a regulator of GPCRs, exerting a tonic brake on GPCR signaling. Inactivating mutations of RSK2 in humans lead to mental retardation, skeletal muscle deformities, and psychosis. Intriguingly, GPCR signaling has been implicated in signaling pathways that regulate brain, bone, and skeletal muscle development (22–26). Alterations of GPCR signaling induced by genetic deletion or inactivation of RSK2 may play a role in the pathogenesis of CLS and may be involved in other disorders manifested by dysmorphogenesis, psychosis, and/or mental retardation.

Materials and Methods

Materials and Constructs. The FLAG-tagged wild-type FLAG-5-HT_{2A} construct was prepared as described (18). Native mouse RSK2 cDNA was subcloned from pMT2-HA-RSK2 (described in ref. 27) into the vector pcDNA3 (Invitrogen) to create the vector RSK2. To construct a viral vector for the expression of RSK2, bases 1938–1940 of the vector RSK2 were first mutated from TTC to CAG by using the Stratagene Quick Change Site-Directed Mutagenesis Kit to remove an EcoRI site at position 1935 of the wild-type mouse RSK2 sequence, while maintaining amino acid identity, to create the vector pRSK2-EcoRI-REM. The RSK2 insert of pRSK2-EcoRI-REM was then subcloned into the EcoRI and SalI sites of pBABE-puro (28) to create pBABE-RSK2-EcoRI-REM. All constructs were verified by automated full-length sequencing (Cleveland Genomics, Cleveland).

HEK-293, HEK-293T, HEK-293TS, and C6 glioma cells were from the American Type Culture Collection (Manassas, VA). [^{3}H]myo-inositol (21.0 Ci/mmol) (1 Ci = 37 GBq) and [^{3}H]ketanserin (76.0 Ci/mmol) were from New England Nuclear. [^{32}P]orthophosphate was obtained from Amersham Pharmacia Biosciences. ATP, bradykinin, chlorpromazine, 5-HT, M2 monoclonal anti-FLAG antibody, polyclonal anti-FLAG antibody, and anti-FLAG M2 agarose beads were from Sigma. The polyclonal antibody (ct-2A) against the C terminus of the 5-HT_{2A} receptor (29) was a gift from Jon Backstrom (Vanderbilt University, Nashville, TN). Additional antibodies were from the following sources: polyclonal goat anti-RSK2, monoclonal anti-RSK2, and polyclonal rabbit anti-$G_{\alpha q}$ antibodies (Santa Cruz Biotechnology); rabbit polyclonal anti-RSK2 antibody (Upstate Biotechnology, Lake Placid, NY); polyclonal rabbit anti-GFP antibody (Abcam, Ltd., Cambridge, U.K.); mouse monoclonal anti-5-HT_{2A} antibody (PharMingen); goat anti-rabbit horseradish peroxidase (HRP) and horse anti-goat HRP secondary antibodies (Vector Laboratories); goat anti-rabbit Alexa Fluor 488 secondary antibody (Molecular Probes); and goat anti-mouse CY3 secondary antibody (Jackson ImmunoResearch).

Cell Culture, Transfection, and Stable Line Production. HEK-293 cells, HEK-293T cells, HEK-293-TS cells, RSK2 wild-type mouse fibroblasts (RSK2+/+), and RSK2 knockout mouse fibroblasts (RSK2−/−) were maintained in DMEM supplemented with 10% FBS/1 mM sodium pyruvate/penicillin (100 units/ml)/streptomycin (100 mg/ml) (GIBCO/BRL) at 37°C and 5% CO_2. Transfections and all further manipulations were as detailed (18, 30). RSK2 and FLAG-5-HT_{2A} amphotrophic retroviruses were produced and infections carried out as described (31). Stable lines were established and maintained by selection in DMEM containing 6 μg/ml puromycin.

Western Blotting, Immunoprecipitation, and Cell Surface Biotinylation. Coimmunoprecipitation and immunoblotting were performed as detailed (18, 30). A monoclonal mouse RSK2 antibody (Santa Cruz Biotechnology) and protein A/G agarose were used to immunoprecipitate RSK2 from C6 glioma cells and from rat brain synaptic membrane preparations. Rat brain synaptic membranes were prepared from rat frontal cortex as described (30). Cell surface biotinylation was performed as described (32).

Immunohistochemistry and Confocal Microscopy. For immunohistochemical studies, rats were perfused with 4% paraformaldehyde, prefrontal cortex sections were prepared, and immunohistochemical localization was done as described (33). Sections were incubated in a mixture of a mouse monoclonal 5-HT_{2A} antibody (Pharmingen; 1:1,000) and a rabbit polyclonal RSK2 antibody (Upstate Biotechnology; 1:100), with subsequent incubation in the secondary antibodies goat anti-rabbit Alexa Fluor 488 (1:400; Molecular Probes) and goat anti-mouse CY3 (1:1250; Jackson ImmunoResearch). Dual-label immunofluorescence confocal microscopy was done as described (18, 30).

Second-Messenger Studies. RSK2+/+ and RSK2−/− fibroblasts were split at 40,000 cells per well into 24-well plates for PI hydrolysis assays and adenylate cyclase assays or at 120,000 cells per well into six-well plates for ERK1/2 phosphorylation assays, in DMEM supplemented with 5% dialyzed FCS, and then serum-starved for 15 h before experimentation. The cells were then prepared for PI hydrolysis studies, for adenylate cyclase assays, or for measurements of ERK1/2 phosphorylation, as described (18, 30, 36). All studies were replicated at least three times and analyzed by nonlinear regression by using PRISM 4.03 software (GraphPad, San Diego). Statistical significance of the data was determined by two-tailed paired t test and was defined as $P < 0.05$.

We thank Dr. Jon Backstrom (Vanderbilt University Medical Center) for generously providing the ct-2A antibody, Dr. Allison Limpert for insight and critical reading of our manuscript, and Dr. Gary Landreth for insightful comments. We thank Konstantina Angelis and the laboratory of Dr. Edward Stavnezer for technical expertise in quantitative RT-PCR. This research was supported by the Gene Expression Array Core Facility of the Comprehensive Cancer Center of Case Western Reserve University; University Hospitals of Cleveland Grant P30 CA43703; National Research Service Award predoctoral fellowship F31MH67435 (to D.J.S.); National Institutes of Health Grants R01MH51635, R01MH61887, and K02MH01366; the National Institute of Mental Health Psychoactive Drug Screening Program (to B.L.R.); and a National Alliance for Research on Schizophrenia and Depression Young Investigator Award (to W.K.K.).

1. Armbruster, B. N. & Roth, B. L. (2005) *J. Biol. Chem.* **280,** 5129–5132.
2. Roth, B. L., Sheffler, D. J. & Kroeze, W. K. (2004) *Nat. Rev. Drug Discov.* **3,** 353–359.
3. Roth, B. L., Baner, K., Westkaemper, R., Siebert, D., Rice, K. C., Steinberg, S., Ernsberger, P. & Rothman, R. B. (2002) *Proc. Natl. Acad. Sci. USA* **99,** 11934–11939.
4. Elphick, G. F., Querbes, W., Jordan, J. A., Gee, G. V., Eash, S., Manley, K., Dugan, A., Stanifer, M., Bhatnagar, A., Kroeze, W. K., *et al.* (2004) *Science* **306,** 1380–1383.
5. Lefkowitz, R. J. & Shenoy, S. K. (2005) *Science* **308,** 512–517.
6. Hanauer, A. & Young, I. D. (2002) *J. Med. Genet.* **39,** 705–713.
7. Frodin, M. & Gammeltoft, S. (1999) *Mol. Cell Endocrinol.* **151,** 65–77.
8. Husi, H., Ward, M. A., Choudhary, J. S., Blackstock, W. P. & Grant, S. G. (2000) *Nat. Neurosci.* **3,** 661–669.
9. Thomas, G. M., Rumbaugh, G. R., Harrar, D. B. & Huganir, R. L. (2005) *Proc. Natl. Acad. Sci. USA* **102,** 15006–15011.
10. Niethammer, M., Kim, E. & Sheng, M. (1996) *J. Neurosci.* **16,** 2157–2163.
11. Harrison, P. J. & Weinberger, D. R. (2005) *Mol. Psychiatry* **10,** 40–68.
12. Trivier, E., De Cesare, D., Jacquot, S., Pannetier, S., Zackai, E., Young, I., Mandel, J. L., Sassone-Corsi, P. & Hanauer, A. (1996) *Nature* **384,** 567–570.
13. Dufresne, S. D., Bjorbaek, C., El-Haschimi, K., Zhao, Y., Aschenbach, W. G., Moller, D. E. & Goodyear, L. J. (2001) *Mol. Cell. Biol.* **21,** 81–87.
14. Bruning, J. C., Gillette, J. A., Zhao, Y., Bjorbaeck, C., Kotzka, J., Knebel, B., Avci, H., Hanstein, B., Lingohr, P., Moller, D. E., *et al.* (2000) *Proc. Natl. Acad. Sci. USA* **97,** 2462–2467.
15. Josselyn, S. A., Shi, C., Carlezon, W. A., Jr., Neve, R. L., Nestler, E. J. & Davis, M. (2001) *J. Neurosci.* **21,** 2404–2412.
16. Gray, J. A., Compton-Toth, B. A. & Roth, B. L. (2003) *Biochemistry* **42,** 10853–10862.
17. Sorensen, S. M., Kehne, J. H., Fadayl, E. M., Humphreys, T. M., Ketteler, H. J., Sullivan, C., Taylor, V. L. & Schmidt, C. J. (1993) *J. Pharmacol. Exp. Ther.* **266,** 684–691.
18. Xia, Z., Gray, J. A., Compton-Toth, B. A. & Roth, B. L. (2003) *J. Biol. Chem.* **278,** 21901–21908.
19. Bockaert, J., Fagni, L., Dumuis, A. & Marin, P. (2004) *Pharmacol. Ther.* **103,** 203–221.
20. Hunter, A. G. (2002) *Am. J. Med. Genet.* **111,** 345–355.
21. Steinberg, S. F. (2005) *Mol. Pharmacol.* **67,** 2–11.
22. Pierce, K. L., Premont, R. T. & Lefkowitz, R. J. (2002) *Nat. Rev. Mol. Cell. Biol.* **3,** 639–650.
23. Cheung, K. K., Ryten, M. & Burnstock, G. (2003) *Dev. Dyn.* **228,** 254–266.
24. Pagel, C. N., de Niese, M. R., Abraham, L. A., Chinni, C., Song, S. J., Pike, R. N. & Mackie, E. J. (2003) *Bone* **33,** 733–743.
25. de Niese, M. R., Chinni, C., Pike, R. N., Bottomley, S. P. & Mackie, E. J. (2002) *Exp. Cell Res.* **274,** 149–156.
26. Chinni, C., de Niese, M. R., Tew, D. J., Jenkins, A. L., Bottomley, S. P. & Mackie, E. J. (1999) *J. Biol. Chem.* **274,** 9169–9174.
27. Zhao, Y., Bjorbaek, C. & Moller, D. E. (1996) *J. Biol. Chem.* **271,** 29773–29779.
28. Morgenstern, J. P. & Land, H. (1990) *Nucleic Acids Res.* **18,** 1068.
29. Backstrom, J. R. & Sanders-Bush, E. (1997) *J. Neurosci. Methods* **77,** 109–117.
30. Bhatnagar, A., Sheffler, D. J., Kroeze, W. K., Compton-Toth, B. & Roth, B. L. (2004) *J. Biol. Chem.* **279,** 34614–34623.
31. Elenbaas, B., Spirio, L., Koerner, F., Fleming, M. D., Zimonjic, D. B., Donaher, J. L., Popescu, N. C., Hahn, W. C. & Weinberg, R. A. (2001) *Genes Dev.* **15,** 50–65.
32. Willins, D. L., Berry, S. A., Alsayegh, L., Backstrom, J. R., Sanders-Bush, E. & Roth, B. L. (1999) *Neuroscience* **91,** 599–606.
33. Bubser, M., Backstrom, J. R., Sanders-Bush, E., Roth, B. L. & Deutch, A. Y. (2001) *Synapse* **39,** 297–304.